Nanoscale

PAPER

View Article Online
View Journal | View Issue

Cite this: *Nanoscale*, 2015, **7**, 12000

Luminescent supramolecular soft nanostructures from amphiphilic dinuclear Re(I) complexes†

Cristina Cebrián,‡§[a] Mirco Natali,§[b] Davide Villa,§[c] Monica Panigati,*[c] Matteo Mauro,*[a,d] Giuseppe D'Alfonso[c] and Luisa De Cola*[a]

Received 14th March 2015,
Accepted 12th June 2015

DOI: 10.1039/c5nr01668a

www.rsc.org/nanoscale

Luminescent metallo-surfactants based on highly emissive dinuclear Re(I) complexes have been synthesized combining the peculiar photophysical behaviour of this class of neutral hydrophobic complexes with new properties imparted by hydrophilic chains anchored on the coordinated chromophoric ligand. In solution, the resulting neutral amphiphiles tend to self-assembly in soft structures. The aggregation properties have been thoroughly investigated in dioxane-water mixtures, where all the complexes assembly in globular-like supramolecular architectures with well-defined size (hydrodynamic diameter = 200–400 nm). The morphology of these nano-objects has been completely characterized with Dynamic Light Scattering (DLS) analysis, Scanning Transmission Electron Microscopy (STEM) and cryo-TEM to determine the size, polydispersity, and stability of the nanoparticles in relationship with the structure of the metallo-surfactants. The photophysical properties of both the isolated metal complexes and their aggregates have been investigated by means of UV-Vis absorption, steady-state and time-resolved emission spectroscopy. Noteworthy, the self-assembly properties of the reported luminescent rhenium metallo-amphiphiles can be modulated by solvent polarity. Even more importantly, such aggregation process yielded a small hypsochromic shift of the emission energy accompanied by a sizeable elongation of the excited-state lifetime and an enhancement of the photoluminescence quantum yield, reaching a remarkably high value of 0.20 despite the air-equilibrated aqueous condition. The presented findings endorse novel possibilities for the efficient use of soft-nanostructures based on metallo-amphiphiles in dual (electron and optical microscopy) bio-imaging applications and theranostics where the non-covalent nature of the intermolecular interactions would offer the powerful and unique possibility to reversibly assemble and disassemble imaging agents.

Introduction

Supramolecular structures formed by the self-assembly of smaller entities, either molecules or part of them, are attracting growing interest in several research areas such as chemistry, biology, biomedical engineering, nanochemistry, materials science and physics.[1] Indeed, self-assembled systems such as bilayers, liposomes, membranes, enzymes and DNA, to cite some, play a pivotal role for the correct functioning and evolution of biological entities.[2]

Self-assembly represents not only a fundamental research topic but also a very appealing and easier approach for the fabrication of ordered functional structures and materials, which otherwise would require longer and more classical covalent chemistry methods. The long-range order arising from the molecular self-organization is of great and growing interest as *e.g.* for improving some of the charge transport and emission properties of electro-active materials used in (opto)electronics,[3] or even allowing novel functions not present in the non-assembled parental components.[4]

[a]*ISIS & icFRC, Université de Strasbourg & CNRS, 8 rue Gaspard Monge, 67000 Strasbourg, France. E-mail: mauro@unistra.fr, decola@unistra.fr; Fax: +33 (0)368855242; Tel: ++33 (0)368855220*
[b]*Dipartimento di Scienze Chimiche e Farmaceutiche, Università di Ferrara, and Centro Interuniversitario per la Conversione Chimica dell'Energia Solare (SOLARCHEM), sez. di Ferrara, Via Fossato di Mortara 17-19, 44121 Ferrara, Italy*
[c]*Department of Chemistry, Università degli Studi di Milano and Milan Unit of INSTM, Via Golgi 19, 20133 Milano, Italy. E-mail: monica.panigati@unimi.it; Fax: +39 0250314405; Tel: +30 0250314352*
[d]*University of Strasbourg Institute for Advanced Study (USIAS), 5 allée du Général Rouvillois, 67083 Strasbourg, France*

†Electronic supplementary information (ESI) available: Detailed synthetic procedures, chemical characterization, instrumentation, additional photophysical and electron microscopy data. See DOI: 10.1039/c5nr01668a

‡Current address: Institut de Chimie, Physique et Matériaux (ICPM), Université de Lorraine, 1 Boulevard François Aragó, 57070 Metz (France).
§C.C., M.N. and D.V. contributed equally to this work.

Hence, objects with controlled shape and size can be built up taking advantage of supramolecular weaker interactions as for instance recognition among complementary-designed molecules, coordination and hydrogen bonds, π–π, metallophilic, hydrophobic/hydrophilic and van der Waals interactions and the delicate equilibrium between those.[1]

In addition, self-assembled nano-materials can be functionalized for a wide range of applications spanning from biomedicine, *e.g.* diagnosis and sensing,[5] drug delivery,[6] regenerative medicine,[7] environmental science,[8] and catalysis.[8a,b,9]

While supramolecular assembling of functional architectures in organic solvent is widely studied,[10] a comprehensive understanding and control of supramolecular entities in a more competitive and biological relevant environment such as water, towards the precise control of their morphology and properties, is still a challenge which requires careful molecular design.[11] To this respect, amphiphilic molecules are amongst the most powerful building blocks for promoting aqueous-based self-assembly.[12] Aiming at merging the rich physicochemical properties introduced by luminescent and electroactive metal complexes, with the amphiphilic features that can be imparted by organic moieties, namely metallo-surfactants, have also been investigated in recent years.[13]

Properly designed luminescent transition metal complexes possess tunable emission color, high photoluminescence quantum yield and emitting excited states generated by spin-forbidden transitions.[14] However, the long-lived luminescent triplet state represents a severe drawback in aerated solution conditions since the dioxygen can efficiently quench the emission under diffusion control. Therefore, for application in which oxygen-free condition cannot be achieved the use of phosphorescent metal complexes is often a problem rather than an advantage.[15] Finding ways to protect and shield such triplet excited-state from quenchers would blossom their efficient application in fields like bio-imaging and photo-catalysis. Most of the strategies applied to circumvent this problem rely on the creation of dendritic structures,[16] the encapsulation in solid nanoparticles[17] or isolation in porous materials.[18]

A different approach is to allow the complexes to assemble into supramolecular structures, as for instance micelles or vesicles, by transforming them in metallosurfactant and favor isolation because of their self-assembly properties. To date, most of the reported metallo-surfactant systems were charged in nature and based on Ru(II),[19] Ir(III),[13b,19a] Pt(II)[20] complexes and, to a lesser extent, Au(I)[21] and Re(I)[22] derivatives. Only very recently metallo-surfactants based on neutral either iridium[13b,23] or platinum[24] compounds have been reported in which the metal-containing moiety represents the hydrophobic head. This is despite the fact that neutral complex would favor closer interactions and tighter packing than in the charged counterparts. Indeed, in the latter case a frustrated growth might take place as a consequence of the higher electrostatic repulsion,[21a,25] yielding to usually less stable aggregates. Under certain conditions, once dissolved in water or in highly polar solvents these neutral amphiphilic complexes give rise to aggregates in which the polar organic tail is exposed to the solvent and the luminescent hydrophobic complex is embedded inside the core, thus providing assemblies with better emissive properties than the non-assembled parental components.

Encouraged by our recent results on highly luminescent dinuclear rhenium complexes bearing diazine ligands and their application in bio-imaging[26] and organic light emitting diodes (OLEDs),[27] as well as by the striking aggregation-induced emission enhancement (AIEE) effect observed and deeply studied for some relative derivatives,[27c,28] we investigated the possibility to form self-assembled soft structures based on such complexes. To this end, we have designed non-ionic dinuclear rhenium-complexes bearing polar and apolar pendants with different lengths.

Herein, we report on the design and preparation of these molecules, jointly with the study of their self-aggregation under the steady increase of solvent mixture polarity and non-solvent (water) content. Photophysical techniques are employed to demonstrate the gain in emission efficiency on going from the non-interacting (solvated) molecules to soft nano-aggregates. A combination of size and morphological analyses describes the obtained supramolecular nano-aggregates. As it will be hereafter shown, the length of both hydrophilic and hydrophobic moieties, the nature of the latter, and the modulation of the polarity of the solvent mixture have profound influence on the self-assembly process of the metallo-surfactants and on the photophysical properties of the so-formed nano-aggregates. In these novel derivatives, the well-tailored aggregation process induces a strong enhancement of the photophysical properties, which represents, to the best of our knowledge, the first examples of neutral metallo-amphiphiles with unprecedently high photoluminescence quantum yield (PLQY) and few μs-long excited-state lifetime in aqueous air-equilibrated condition.

Such unique properties associated with the formation of soft nano-aggregates, together with the high electron density contrast offered by the self-assembled metallo-amphiphiles, will pave the way towards a novel set of efficient bimodal biological imaging agents with well defined morphological and better photophysical, and contrast imaging properties,[29] where the non-covalent nature of the intermolecular interactions would also offer the powerful possibility to reversibly assemble and disassemble functional molecules favouring internalization and draining.

Molecular design

The new rhenium(I) complexes **1–4** here investigated are sketched in Chart 1. They were designed to possess amphiphilic character in which the luminescent neutral dinuclear rhenium core represents the hydrophobic head, while the hydrophilic part is provided by the polar tail, either as a tri- or a tetra-ethylene glycol chain. Such two moieties, namely the rhenium complex and the hydrophylic chain, were linked together by means of a different lipophilic group (either an alkyl chain or a phenyl ring), which was varied in order to evaluate the effect of rigidity, steric hindrance and degree of lipophilic character onto the aggregation properties of the

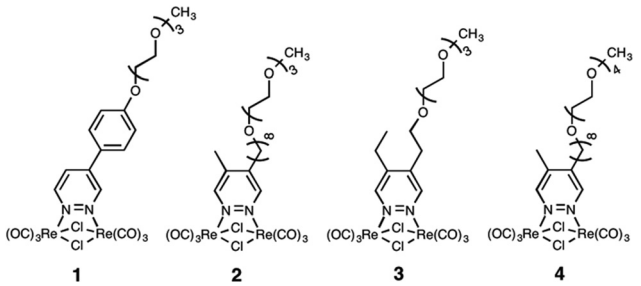

Chart 1 Chemical structure and numbering of the amphiphilic rhenium complexes investigated.

molecules as well as the photophysical and morphological features of the aggregates.

In particular, compound **1** was designed to bear some resemblance to non-ionic surfactants of the Triton-X100 family. Complexes **2** and **3**, bearing the same polar tail but different lipophilic alkyl substituents on the diazine ligand, were prepared to compare the aggregation properties of metallo-surfactants with those of compound **1**, containing an aryl spacer. Finally, complex **4** was prepared, which only differs from **2** for the presence of an additional ethoxy unit, because it is known that the self-assembly properties of surfactants strictly depend on the delicate balance between polar and apolar moieties. Alkyl substituents were inserted in both the 4 and 5 positions of the diazine ligands in complexes **2–4**, since it is known that this might result in dinuclear Re(I) complexes with much higher photoluminescence quantum yields.[27,28,30]

The complexes were synthesized in the three-step procedure shown in Scheme 1 for **1** and Scheme 2 for **2–4**. Further details

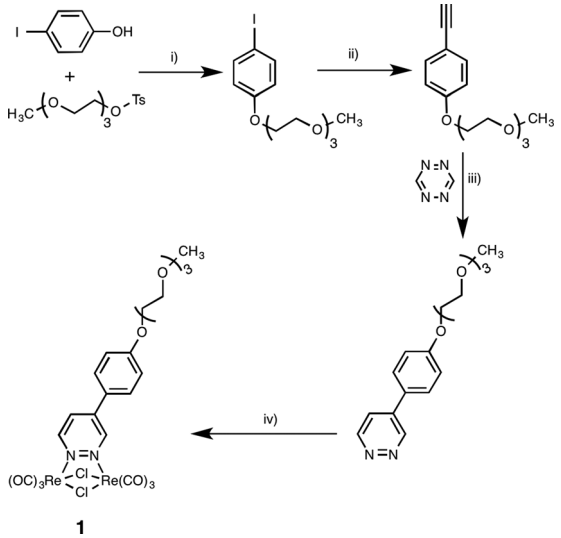

Scheme 1 General schematic synthetic pathway followed for the preparation of the luminescent rhenium metallo-amphiphile **1**. Reaction conditions: (i) K_2CO_3, Bu_4NBr, 90 °C; (ii) ethynyltrimethylsilane, $Pd(PPh_3)_4$, CuI, iPr_2NH, 90 °C; (iii) $NH_2NH_2{\cdot}H_2O$, formamidine acetate, room temperature; (iv) $[Re(CO)_5Cl]$, toluene, reflux.

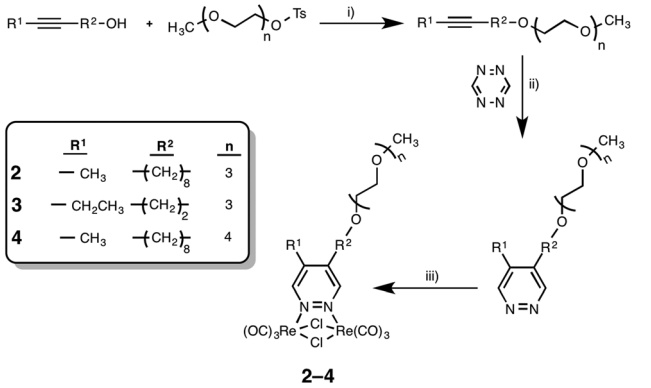

Scheme 2 General schematic synthetic pathway followed for the preparation of the luminescent rhenium metallo-amphiphiles **2–4**. Reaction conditions: (i) NaH, THF, 0 °C → room temperature; (ii) $NH_2NH_2{\cdot}H_2O$, formamidine acetate, room temperature; (iii) $[Re(CO)_5Cl]$, toluene, reflux.

can be found in the ESI.† At first, commercial alkynols were deprotonated with NaH and reacted with the tosyl derivatives of oligo-ethylene glycol monomethyl ethers according to the Williamson's S_N2 reaction.[31] The functionalized alkynes were used for the synthesis of the diazine-based ligands accordingly to the literature procedure which involves an inverse-type [4 + 2] Diels–Alder cycloaddition reaction between the electron-poor 1,2,4,5-tetrazine and an appropriate electron-rich dienophile, *i.e.* the functionalized alkynes, with N_2 loss.[32] Following our previously reported procedure,[30] the amphiphilic luminescent complexes **1–4** were prepared by refluxing $[Re(CO)_5Cl]$ with 0.5 equivalents of the corresponding 4,5-disubstituted-1,2-diazine in toluene solution. Finally, they were obtained as pure yellow-orange powders in high isolated yields after purification by column chromatography.

Results and discussion

Photophysical characterization of the monomeric species

Investigation of complexes **1–4** were performed in dilute (concentration = 1.0×10^{-5} M) toluene solution where aggregation is expected to be negligible and the complexes to behave as solvated isolated monomeric species. The most relevant photophysical data are listed in Table 1 and the corresponding absorption and emission spectra displayed in Fig. 1. The electronic absorption spectra of compounds **1–4** in toluene (Fig. 1, black traces) display low-energy broad band in the region between 330 and 450 nm that can be assigned to the $Re_2(\delta)L(\pi) \rightarrow L(\pi^*)$ spin-allowed metal-to-ligand charge transfer, ^{1}MLCT, transition by comparison with parental derivatives[27,28,30] and mononuclear rhenium tricarbonyl complexes.[33] In particular, introduction of an aromatic substituent on the diazinic ring in compound **1** induces a bathochromic shift of a degree of 30–40 nm and a three-fold increase of the molar absorption coefficient ($\varepsilon = 2.37 \times 10^4$ M^{-1} cm^{-1} at $\lambda_{abs} = 400$ nm) with

Table 1 Photophysical data of metallo-amphiphiles **1–4** in toluene solution at concentration of 1.0×10^{-5} M

Sample	λ_{abs} ($\varepsilon \times 10^3$) [nm (M^{-1} cm^{-1})]	λ_{em}[a] [nm]	λ_{em}[c] [nm]	τ[a,d] [μs]	τ[b,d] [μs]	τ[c,e] [μs]	PLQY[a,f]	PLQY[b,f]
1	399 (23.7)	592	526, 557	0.61	5.9	185 (63%), 685 (37%)	0.02	0.22
2	368 (7.7)	550	497	0.44	4.3	28.8	0.04	0.39
3	364 (7.6)	550	496	0.46	4.1	27.3	0.04	0.41
4	356 (7.3)	552	497	0.44	4.3	28.4	0.04	0.34

[a] At room temperature in air-equilibrated toluene. [b] At room temperature in degassed toluene. [c] At 77 K in a 2-MeTHF rigid matrix. [d] Excitation wavelength at 405 nm for **1** and at 375 nm for **2–4**, analysis wavelength at 590 nm for **1** and 550 nm for **2–4**. [e] Excitation wavelength at 405 nm, analysis wavelength at 530 nm for **1** and 500 nm for **2–4**. [f] Calculated with relative method using $Ru(bpy)_3Cl_2$ as relative standard for **1** (PLQY = 0.04 in air-equilibrated water) and *fac*-Ir(ppy)$_3$ for **2–4** (PLQY = 0.97 in degassed 2-MeTHF).

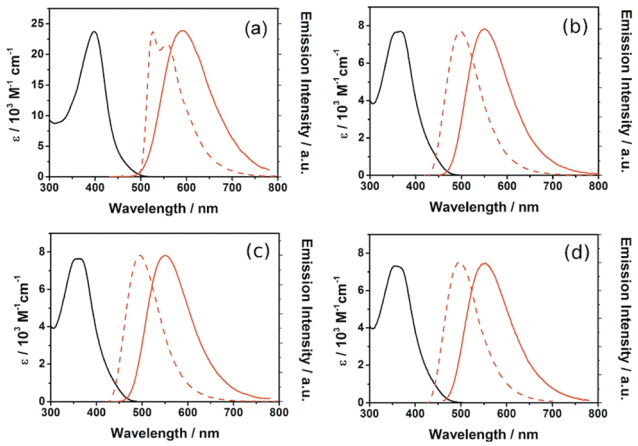

Fig. 1 Absorption (black traces) and emission (red solid traces) spectra of compound **1** (a), **2** (b), **3** (c) and **4** (d) in dilute (1.0×10^{-5} M) toluene solutions at room temperature (λ_{exc} = 400 and 380 nm, for **1** and **2–4**, respectively) and emission spectra in 2-MeTHF glassy matrix at 77 K (λ_{exc} = 400 and 380 nm, for **1**, **4** and **2–3**, respectively, red dashed traces). For all four derivatives, emission spectra are found to be independent of excitation wavelength.

respect to complexes bearing alkyl substituents, namely **2–4** (ε = 7.3–7.7 × 10^3 M^{-1} cm^{-1} at λ_{abs} *ca.* 360 nm) because of the presence of a more π-conjugated system.

Upon excitation in the range 340–400 nm, all samples in toluene show rather intense broad and featureless emission at room temperature that falls in the green-yellow region of the visible spectrum and arises from an emitting excited state with mainly triplet MLCT character.[27,28,30] The photoluminescence spectra of compounds **1–4** are reported in Fig. 1 (red traces). The origin of such very large Stokes shift (>8000 cm^{-1}) observed for luminescent rhenium(I) tricarbonyl complexes has been already widely investigated elsewhere.[34] The emission profile recorded for compound **1** mirrors the behaviour observed for the corresponding absorption spectrum, since it displays a bathochromic shift of *ca.* 50 nm with respect to the emission maxima recorded for **2–4**. This finding is consistent with the lower energy of the emitting excited state of complex **1**, which bears a more π-conjugated system, when compared to that of the derivatives **2–4**. Degassed samples of the complexes in toluene showed PLQY values as high as 0.22 for **1**, and in the range 0.34–0.41 for the complexes **2–4** (see Table 1). Similarly to the parental complexes previously reported by our group,[27,28,30] the excited state lifetimes are in the range 4.1–4.3 μs for derivatives **2–4**, while a slightly slower mono-exponential decay kinetics (τ = 5.9 μs) is recorded for **1**, as a consequence of the more extended delocalization which involves the phenyl ring present as spacer between the diazine ring and the oligo-ethylene glycol chain. Indeed, the lowest luminescent excited state is a ^{3}MLCT involving the diazine and the 3-phenyl substituted diazine for **2–4** and **1**, respectively.

Complexes **2–4** exhibit lower PLQY and shorter excited state lifetimes compared to the analogue compounds possessing shorter chains.[27b,c] Such worse performance can be due to radiationless deactivations caused by the vibrational modes of both the long alkyl and the oligoethylene glycol chains. Indeed the radiative kinetic constants, $k_r \times \eta_{ISC}$, (where $\eta_{ISC} \approx 1$ is the efficiency of the singlet-to-triplet intersystem crossing process)[35] by means of the relationship $k_r \times \eta_{ISC}$ = PLQY/τ, gave values in the range 0.8–1.0 × 10^5 s^{-1} which match rather well those observed for the non-pegylated complexes.[27,28,30]

Going from fluid solution (room temperature) to 2-MeTHF glassy matrix at 77 K (Fig. 1, dashed red traces), the photoluminescence spectra of **2–4** maintain the structureless profile with a concomitant hypsochromic shift of the maximum (*ca.* 50 nm) due to the so-called rigidochromic effect,[36] which arises from the increase in energy of the emitting ^{3}MLCT state less stabilized by the lack of solvent mobility, and a prolongation of the excited state lifetime, falling now in the range 27.3–28.8 μs.

On the other hand, for complex **1** the 77 K emission spectrum displays a hypsochromically-shifted profile with the clear appearance of a vibronic structure (λ_{em} = 526 and 557 nm), indicating a larger contribution of the triplet-manifold ligand centred (^{3}LC) character to the emitting state. We expect that the presence of a larger conjugated ligand (phenyl-diazine) possessing a lower energy level (LUMO), can favour equilibrium between the ^{3}LC and the ^{3}MLCT states. Indeed the destabilization of the MLCT in rigid matrix rise the energy of this state that can efficiently mix with the long-lived ligand centred triplet state. This hypothesis is corroborated by the fact that compound **1** shows a bi-exponential decay kinetics

with a short (τ_1 = 185 μs, 63%) and a longer (τ_2 = 685 μs, 37%) component.[37]

Aggregation study

Complexes **1–4** were carefully designed to display amphiphilic character due to the presence in the same molecule of an apolar head, namely the dinuclear rhenium complex with the alkyl chains, and a pendant oligo-ethylene oxide chain acting as the hydrophilic tail. Upon certain conditions, such amphiphilic nature is predicted to strongly induce self-organization of the phosphorescent molecules in solution. Different medium polarity and/or presence of solvent/non-solvent mixtures at variable ratio are expected to strongly influence aggregation properties and aggregates features. The formation of assemblies of complexes **1–4** is also expected to cause a change in the photophysical properties.

In order to gain insights onto the aggregation properties of the oligo-ethylene oxide-containing neutral Re(I) surfactants, the photophysical properties of **1–4** have been thoroughly studied jointly with morphological analyses on freshly prepared samples in dioxane/water solvent mixture upon steady variation of the water content from 0% (*i.e.*, pure dioxane) up to 95%. The use of a dioxane/water mixture, as the solvent and the non-solvent, respectively, is very convenient for two-fold reasons, in particular as (i) the miscibility of the two solvents is always complete at all desired ratios and (ii) the variation of the dielectric constant is almost linear within a wide range of dioxane/water compositions, allowing for a high degree of modulation and control of the polarity.[38] The concentration of complexes **1–4** has been kept constant (5.0×10^{-5} M) over the whole investigation in order to directly evaluate only the effect of the variation in polarity onto the association equilibria.

The most relevant photophysical data obtained in the different dioxane/water mixtures for the metallo-amphiphile **1** and **3** are summarized in Tables 2 and 3, respectively, while the data recorded for the derivatives **2** and **4** are reported in Tables S1 and S2 of the ESI,† respectively. For compound **3**, the absoption and emission spectra are displayed in Fig. 2,

Table 2 Photophysical data of samples of the metallo-surfactant **1** at concentration of 5.0×10^{-5} M in air-equilibrated dioxane/water mixtures

Dioxane/ water ratio	λ_{em}[a] [nm]	τ[b] [μs]	PLQY[c]
100/0	603	0.54	0.02
80/20	605	0.53	0.01
60/40	610	0.55	0.02
40/60	615	0.53	0.02
20/80	591	0.83 (27%), 4.3 (73%)	0.07
10/90	587	6.2	0.10
5/95	587	7.1	0.11

[a] At room temperature, excitation wavelength at 430 nm. [b] At room temperature, excitation wavelength at 405 nm, analysis wavelength at 600 nm. [c] Absolute quantum yields by means of an integrating sphere setup.

Table 3 Photophysical data of samples of the metallo-surfactant **3** at concentration of 5.0×10^{-5} M in air-equilibrated dioxane/water mixtures

Dioxane/ water	λ_{em}[a] [nm]	τ[b] [μs]	PLQY[c]
100/0	562	0.43	0.03
80/20	565	0.45	0.03
60/40	570	0.44	0.03
40/60	573	0.50	0.04
20/80	576	0.57	0.03
10/90	553	2.2	0.13
5/95	550	2.4	0.19

[a] At room temperature, excitation wavelength at 400 nm. [b] At room temperature, excitation wavelength at 405 nm, analysis wavelength at 565 nm. [c] Absolute quantum yields by means of an integrating sphere setup.

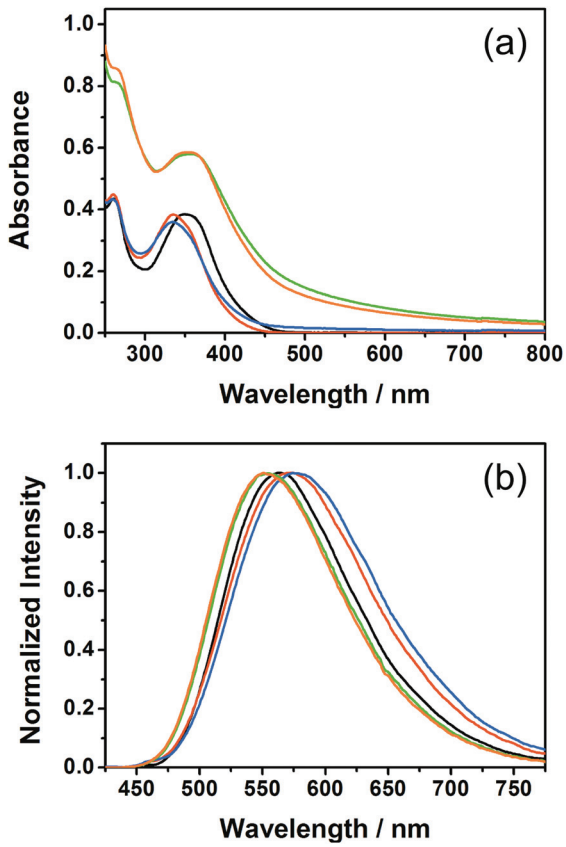

Fig. 2 (a) Absorption spectra and (b) normalized emission spectra obtained for the metallo-surfactant **3** at concentration of 5.0×10^{-5} M in different dioxane/water composition. Color code: 100 : 0 (black), 60 : 40 (red), 20 : 80 (blue), 10 : 90 (green), 5 : 95 (orange). Traces corresponding to 80 : 20 and 40 : 60 dioxane/water have been omitted for sake of clarity. For emission spectra, the samples were excited at λ_{exc} = 400 nm.

while those corresponding to complexes **1**, **2** and **4** are shown in Fig. S1, S2 and S3,† respectively.

It is important to note that, at the chosen concentration, all complexes **1–4** are found to be perfectly soluble in pure

dioxane, where they can be reasonably consider as free monomeric species. Indeed, their spectral features (absorption and emission) and photophysical data, including lifetime and PLQY are comparable with those obtained in dilute toluene solution (see Tables 1 and 2 and black traces in Fig. 2 and S1–S3 of the ESI†).

For all the derivatives, upon increasing water content up to 60% the variation of the maxima in both absorption and emission spectra can be simply ascribed to the increase of dielectric constant of the solvating media.[36a,37c] Indeed, addition of water gives a hyspochromic shift of the ^{1}MLCT band in the absorption spectra (Fig. 2a for **3**, and Fig. S1a, S2a and S3a† for **1**, **2** and **4**, respectively), and a mirroring bathochromic shift of the emission maxima (Fig. 2b for **3**, and Fig. S1b, S2b and S3b† for **1**, **2** and **4**, respectively). The PLQY values remain at 1–3%, which are similar to those measured in pure solvent either dioxane or toluene. Likewise, for samples in such solvent mixtures the recorded lifetimes are also in the range of 0.4–0.5 μs, well corresponding to the radiative decay of the ^{3}MLCT excited state of the monomeric species in air-equilibrated condition.

As soon as water content exceeds 80%, drastic changes on the photophysical properties are observed. The absorption spectra display more intense bands with pronounced tails that extend in the visible region. These changes of the overall photophysical features seem to suggest the formation of aggregates in such solvent mixture. In fact, the presence of a higher baseline in the electronic absorption spectra is consistent with scattering processes, which can be ascribed to the formation of nanosized aggregates, never observed in samples with water content below 80%. Indeed, due to the amphiphilic nature of derivatives **1–4**, it is reasonable to think that in a very polar environment, such as that corresponding to high water content, self-assembly processes occur in which the apolar dinuclear rhenium heads pack close to each other segregating from to the water molecule, while the more polar and hydrophilic oligo-ethylene glycol tails are solvated by water.

The formation of these assemblies causes important effects on the photophysical properties. The emission spectra are displayed in Fig. 2b for **3**, and Fig. S1b, S2b and S3b† for **1**, **2**, and **4**, respectively (see also Tables 2, 3 and Tables S1, S2 of the ESI†). In fact, formation of aggregates induces a hyspochromic shift of a degree of 15–30 nm of the photoluminescence spectral band, which can strongly support the idea that the emitting MLCT state, involving the metal complexes, experiences a less polar environment due to the tighter packing *via* the aggregation process, which thus prevents water to be in direct contact with the dinuclear rhenium heads.

Moreover, as a direct consequence of the efficient packing process and the low diffusion, if any, inside the aggregates, of dioxygen molecules the excited state lifetimes become much longer. Also, as expected the PLQY values sizeably increase up to 0.20 in air-equilibrated condition. Such results can be clearly ascribed to the lack of quenching by O_2 despite the triplet nature of the luminescent excited state and the increase rigidity of the assembly, in comparison with the monomeric

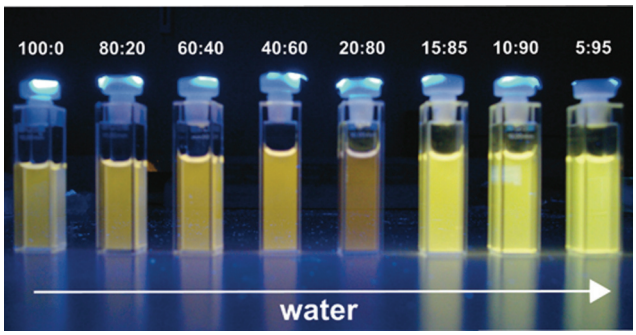

Fig. 3 Picture showing samples of the metallo-sufactant **3** at concentration of 5.0×10^{-5} M in the different dioxane/water solutions upon irradiation with top-bench UV light.

species, that reduce radiationless deactivation pathways. The strong increase of the emission efficiency can be observed even by naked eye as shown in Fig. 3 for samples of the metallo-surfactant **3**, and Fig. S4–S6† for **1**, **2**, and **4**, respectively, in dioxane/water mixtures at different ratio upon UV irradiation.

As abovementioned, steady increase of the lifetimes and PLQY values observed for the metallo-amphiphiles **1–4** at higher water content has been obtained in air-equilibrated solutions. As proof of principle, and in order to evaluate the shielding of the tight aggregate from dioxygen quenching, solutions of compounds **1** and **3** at 10/90 dioxane/water ratio were carefully purged with argon for more than 30 minutes. As can be seen in Tables 2 and 3, in air-equilibrated condition the complexes at 10/90 dioxane/water ratio possess a monoexponential decay with luminescence lifetime of 6.2 μs and 2.2 μs for **1** and **3**, respectively. After deaeration, the samples show only a small increase of the excited-state lifetimes (8.7 and 3.1 μs for **1** and **3**, respectively). This finding suggests the effective shield towards the external environment and the strong gain in terms of emission efficiency that can be easily achieved by exploiting the supramolecular self-assembling of triplet-manifold luminophores.

In order to further confirm the presence of luminescent aggregates based on the metallosurfactants here reported and to deeper investigate the size and morphology of such soft supramolecular aggregates, we have performed dynamic light scattering (DLS) and electron microscopy analyses on the same samples previously investigated by using photophysical techniques. The DLS results are shown in Fig. 4 for derivative **3–4** at 10/90 and 5/95 dioxane : water content and the size and polydispersity listed in Table S3 of the ESI† for all the derivatives.

For all the investigated compounds, DLS data obtained for samples with high water composition, typically above 80%, showed particles sizes with averaged hydrodynamic diameter between 130 and 460 nm, consistent with formation of either vesicular or globular assemblies.[39] In addition, we did not notice any degradation and assemblies resulted stable for several hours in the dioxane/water mixtures.

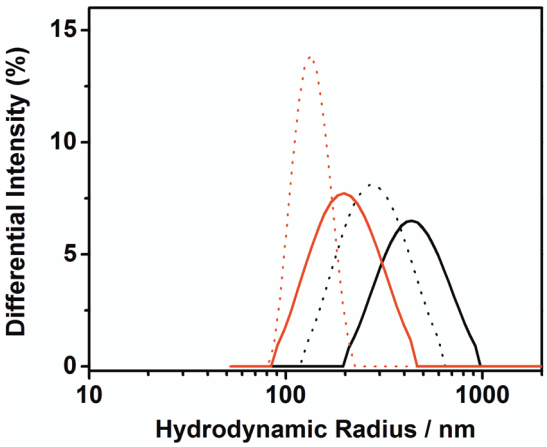

Fig. 4 Hydrodynamic radii distribution obtained by means of DLS analysis of samples of **3** (black traces) and **4** (red traces) at 10 : 90 (solid traces) and 5 : 95 (dotted traces) dioxane : water ratio.

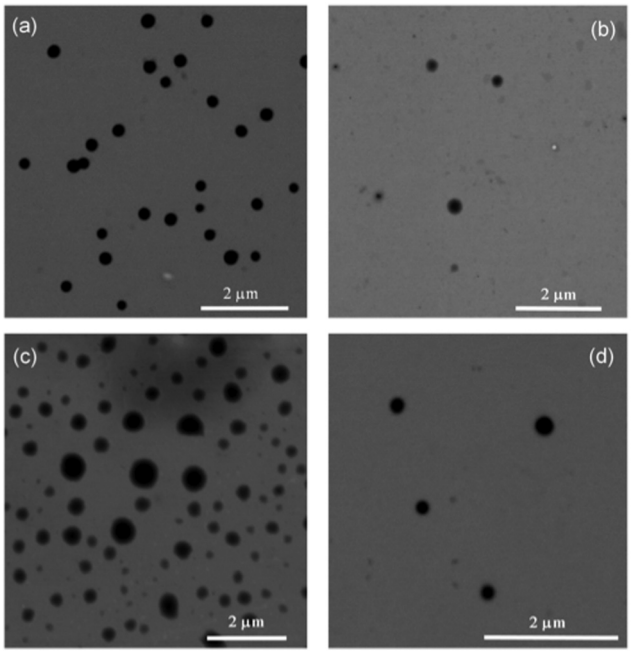

Fig. 5 STEM images of drop-casted samples onto a copper grid at 10/90 dioxane/water ratio of the metallo-amphiphile (a) **1**, (b) **2**, (c) **3**, and (d) **4**, clearly showing the formation of nano-sized soft aggregates.

As it can be observed, the particle size and distribution are strongly dependent on the amount of water present in solution for all the investigated complexes. In particular, (i) at water content between 0–60% no DLS signal corresponding to the formation of aggregates has been recorded for the whole series of compounds **1–4** (until 80% water for **3**), in nice agreement with the spectroscopic data discussed above; (ii) when the water content exceeds to some little extent the threshold value needed for formation of aggregates (*i.e.*, at 80% water for metallo-surfactant **2** and **4**) the samples display a rather non-homogeneus distribution of sizes of the aggregates, as demonstrated by the values of the polydispersity index, PDI, obtained by DLS (see Table S3 of the ESI†). Such findings matches rather well the bi-exponential decays obtained for the same samples during the photophysical measurements (*vide infra*); (iii) as the amount of water is in larger excess with respect to the dioxane fraction and reaches values above 90%, the particle sizes tend to reach a narrow monomodal distribution (see Fig. 4, solid traces), compatible with more defined and homogeneous assemblies; finally, (iv) when the water content is as high as 95%, the size of the nano-aggregates becomes smaller and narrower with respect to 90% water content, as suggested by the smaller hydrodynamic diameter (see Fig. 4). The latter effect can be explained taking into account polarity-driven interactions and an increased hydrophobic effect experienced by the apolar heads at such very high water content. A tighter packing of the neutral metallo-surfactants reduces the surface exposed to the highly polar water-rich environment, thus minimizing repulsive interactions. Overall, the largest and smallest hydrodynamic diameter measured for the 95% water content samples is 295.2 ± 105.5 and 135.6 ± 26.2 nm, respectively, for aggregates formed upon solvent-induced self-assembly process of metallo-surfactant **3** and **4**, respectively.

Formation of ordered soft nanostructures is also confirmed by STEM analysis of drop-casted 10/90 dioxane/water solutions containing metallo-amphiphiles **1–4** at concentration of 1.0×10^{-4} M and after further dilution 1 : 1 with methanol. Fig. 5 displays representative STEM images obtained for these samples.

Electron microscopy analyses clearly revealed the formation of soft nano-sized aggregates. In particular, in the case of derivative **1**, spherical aggregates with homodisperse size distribution can be observed displaying an average diameter of about 300 nm. As far as derivative **2** and **4** are concerned, soft structures with diameters in the same order can be generally observed, even though a minor amount of either smaller or amorphous structures is also present. Finally, comparable with the DLS results, compound **3** displays vesicular or globular structures with larger diameter sizes with measurable average values around 400 nm. As a further proof of the formation of nano-sized soft architecture based on the here reported neutral metallo-amphiphiles, we performed dark-field STEM analysis on samples of derivative **1**. As it can be seen in Fig. S7 of ESI,† the white colour observed undoubtedly demonstrates the presence of heavy rhenium atoms inside the observed nano-structures.

Finally, in order to gain insights onto the aggregates' morphology transmission electron microscopy imaging at cryogenic temperature (cryo-TEM) was carried out on samples of metallo-amphiphile **1** and **3** at concentration of 1.0×10^{-4} M in 10/90 dioxane/water. The micrographs, which are displayed in Fig. 6, confirm the formation of nanosized aggregates with core-shell structural organization corresponding to complex globular-like micelles, in which the inner core is characterized by higher electron density as consequence of accumulation of the heavy atoms-containing apolar heads.

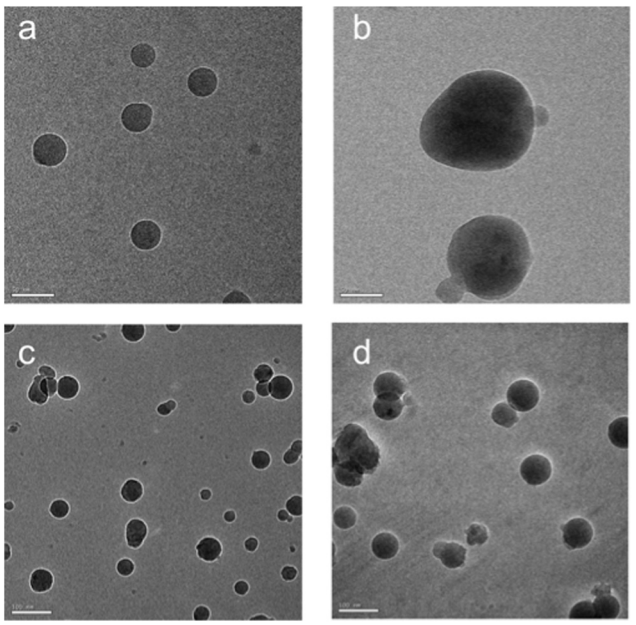

Fig. 6 Cryo-TEM images recorded for 90/10 H_2O : dioxane samples of nanosized aggregates of complex **1** (a, b) and **3** (c, d) at concentration of 1.0×10^{-4} M. Scale bar is 50 and 100 nm for a, b and c, d, respectively.

Overall, from the combination of the results obtained by means of photophysical techniques and morphological analyses we can argue on the structure–properties relationship and in particular on the aggregation capability of metallo-amphiphiles **1–4**. We have demonstrated that a similar aggregation tendency can be observed for compounds **2** and **4**, since their molecular structures only differ for the presence of an additional ethylene oxide unit in **4** in comparison to **2** (four *vs.* three units, respectively). For both complexes, aggregation begins at 80% water content and the formed soft structures display a large variability of size also upon increasing water content up to 95% as supported by the bi-exponential lifetime decays, poor monodispersed distribution observed by DLS and presence of a non-negligible amount of amorphous structures observed by STEM. This behaviour can be probably ascribed to the higher mobility of the chains featuring high degree of conformational freedom, and the rather short length of the chains that prevents the stabilization of the soft structures.

On the other hand, as far as the derivative **3** is concerned, formation of aggregates can only be observed if water content reaches values above 90% (see Tables 3 and S3†). The reason can be likely related to the presence of the shorter apolar alkyl chain (*i.e.*, $-CH_2CH_2-$) that reduces the overall hydrophobicity of the apolar head by comparison with compounds **1**, **2**, and **4**. The hydrophilicity/hydrophobicity ratio is indeed expected to strongly influences the self-assembly properties of metallo-amphiphiles. Nonetheless, soft-structures made by **3** seems to be the largest ones observed within the **1–4** series due to the presence of a shorter linking $-CH_2CH_2-$ chain, which reduce the amount of van der Waals forces and hydrophobic effect needed for the assemblies formation. This finding can be likely ascribed to the steric hindrance exerted by the larger ethyl group present in the fifth position of the diazine ligand, which may actively determine a different supramolecular organization as a consequence of the different molecular packing parameters. However, such differences are beneficial for the packing as reflected in the photophysical properties of the assemblies obtained with **3** that showed the highest values of PLQY (see Table 3).

The best results in terms of packing capability, defined as the amount of water needed for the formation of the aggregate and homogeneity and compactness of the assemblies, is attained for metallo-amphiphile **1**. This efficiency seems to rely on the very different structural composition of this compound with respect to **2–4**. Indeed, the presence of a phenyl group has interesting consequence on the energy and excited state of the emissive state (see above) but also could favour intermolecular stabilization because of the π–π interactions. Indeed, the photophysics of the aggregates for this complex is particularly interesting since despite the hypsochromic shift the emission is still quite low in energy and the excited state lifetime is the longest and more than three-fold longer than the analogous systems that does not posses the phenyl substitution, *e.g.* complex **3**. Interplay of rigidity, conjugation and intermolecular interactions could therefore promote better supramolecular packing.

Conclusions

In conclusion, a series of novel neutral metallo-surfactants based on luminescent dinuclear rhenium complexes is reported and the self-assembly properties thoroughly investigated by means of different photophysical and morphological techniques upon variation of the solvent/non-solvent ratio. It has been found that all the derivatives self-aggregate in dioxane/water mixture at water content higher than 80%. Interesting correlations between the chemical structure of the complexes and their self-organization into well defined and homodisperse soft aggregates are found. The assembly process yields to a strong increase of the PLQY up to 0.20 in air-equilibrated condition. Such values are very close to those recorded for samples of the self-assembled derivatives in Ar-purged condition. Importantly, a concomitant prolongation of the excited state lifetime is achieved, suggesting a strong shielding of the emitters from the environment once the supramolecular assemblies are formed. All these findings will pave the way to the use of neutral luminescent metallo-surfactants in dual-imaging applications, in which high PLQY and high electron density contrast are simultaneously needed.

Acknowledgements

L.D.C. is grateful to the University of Strasbourg, the CNRS, the Région Alsace, the Communauté Urbaine de Strasbourg, the Gutenberg Chair (2011–2012) and to AXA Research funds.

D.V., M.P., G.D., C.C., M.M. and L.D.C. gratefully acknowledge the DAAD-Vigoni project "Nanoscale organization of luminescent complexes for innovative materials". M.N. gratefully acknowledges the Italian MIUR (FIRB RBAP11C58Y "Nano-Solar") for funding and the scholarship from IUSS-1391 Ferrara. The authors gratefully thank Dr Laura Maggini (Unistra) for STEM micrographs and Corinne Crucifix (IGBMC, Unistra) for cryo-TEM analysis.

Notes and references

1 (*a*) J. M. Lehn, *Supramolecular Chemistry*, WILEY-VCH Verlag GmbH, Weinheim, 1995; (*b*) *Supramolecular Chemistry: From Molecules to Nanomaterials*, ed. P. Gale and J. Steed, Wiley-VCH Verlag GmbH & Co. KGaA, Weinheim, 2012; (*c*) *Comprehensive Supramolecular Chemistry*, ed. J. L. Atwood, J. E. D. Davies, D. D. MacNicol, F. Vögtle and J.-M. Lehn, Pergamon, Oxford, 1996; (*d*) G. M. Whitesides, J. P. Mathias and C. T. Seto, *Science*, 1991, **254**, 1312–1319; (*e*) J. M. Lehn, *Science*, 2002, **295**, 2400–2403; (*f*) D. N. Reinhoudt and M. Crego-Calama, *Science*, 2002, **295**, 2403–2407; (*g*) J.-M. Lehn, *Proc. Natl. Acad. Sci. U. S. A.*, 2002, **99**, 4763–4768; (*h*) G. Whitesides and M. Boncheva, *Proc. Natl. Acad. Sci. U. S. A.*, 2002, **99**, 4769–4774.

2 (*a*) S. Brakman, *Biophys. Chem.*, 1997, **66**, 133–143; (*b*) D. Philp and J. F. Stoddart, *Angew. Chem., Int. Ed. Engl.*, 1996, **35**, 1154–1196.

3 (*a*) E. W. Meijer and A. P. H. Schenning, *Nature*, 2002, **419**, 353–354; (*b*) A. P. H. J. Schenning and E. W. Meijer, *Chem. Commun.*, 2005, 3245–3258; (*c*) Y. Yamamoto, T. Fukushima, Y. Suna, N. Ishii, A. Saeki, S. Seki, S. Tagawa, M. Taniguchi, T. Kawai and T. Aida, *Science*, 2006, **314**, 1761–1764; (*d*) D. M. Bassani, L. Jonusauskaite, A. Lavie-Cambot, N. D. McClenaghan, J.-L. Pozzo, D. Ray and G. Vives, *Coord. Chem. Rev.*, 2010, **254**, 2429–2445; (*e*) M. Y. Yuen, V. A. L. Roy, W. L. Lu, S. C. F. Kui, G. S. M. Tong, M. H. So, S. S. Y. Chui, M. Muccini, J. Q. Ning, S. J. Xu and C. M. Che, *Angew. Chem., Int. Ed.*, 2008, **47**, 9895–9899; (*f*) C. A. Strassert, C. H. Chien, M. D. Galvez Lopez, D. Kourkoulos, D. Hertel, K. Meerholz and L. De Cola, *Angew. Chem., Int. Ed.*, 2011, **50**, 946–950; (*g*) J. M. Mativetsky, E. Orgiu, I. Lieberwirth, W. Pisula and P. Samori, *Adv. Mater.*, 2014, **26**, 430–435.

4 (*a*) H. Sirringhaus, P. J. Brown, R. H. Friend, M. M. Nielsen, K. Bechgaard, B. M. W. Langewveld-Voss, A. J. H. Spiering, R. A. J. Janseen, E. W. Meijer, P. Herwig and D. M. de Leeuw, *Nature*, 1999, **401**, 685–688; (*b*) E. Busseron, Y. Ruff, E. Moulin and N. Giuseppone, *Nanoscale*, 2013, **5**, 7098–7140; (*c*) M. Mauro, A. Aliprandi, C. Cebrián, D. Wang, C. Kübel and L. De Cola, *Chem. Commun*, 2014, **50**, 7269–7272.

5 See for instance: (*a*) Z. P. Aguilar, Nanobiosensors, in *Nanomaterials for Medical Applications*, ed. A. Zoraida, Elsevier, ch. 4, 2013; (*b*) *Nanomaterials for Medical Diagnosis and Therapy*, ed. C. S. S. R. Kumar, Wiley-VCH Verlag GmbH & Co. KGaA, Weinheim, 2007.

6 (*a*) O. C. Farokhzad and R. Langer, *ACS Nano*, 2009, **3**, 16–20; (*b*) Y.-B. Lim, K.-S. Moon and M. Lee, *Chem. Soc. Rev.*, 2009, **38**, 925–934.

7 (*a*) T. Dvir, B. P. Timko, D. S. Kohane and R. Langer, *Nat. Nanotechnol.*, 2011, **6**, 13–22; (*b*) K. Rajangam, H. A. Behanna, M. J. Hui, X. Han, J. F. Hulvat, J. W. Lomasney and S. I. Stupp, *Nano Lett.*, 2006, **9**, 2086–2090; (*c*) J. D. Hartgerink, E. Beniash and S. Stupp, *Science*, 2001, **294**, 1684–1688.

8 (*a*) *Metal–Organic Frameworks: Applications from Catalysis to Gas Storage*, ed. D. Farrusseng, Wiley-VCH Verlag GmbH & Co. KGaA, Weinheim, 2011; (*b*) *Functional Metal–Organic Frameworks: Gas Storage, Separation and Catalysis*, ed. M. Schröder, Springer, Berlin Heidelberg, 2010, vol. 293; (*c*) S. Matile, N. Sakai and A. Hennig, Transport Experiments in Membranes, in *Supramolecular Chemistry: From Molecules to Nanomaterials*, ed. P. Gale and J. Steed, Wiley-VCH Verlag GmbH & Co. KGaA, Weinheim, 2012, vol. 2; (*d*) G. T. Noble, R. J. Mart, K. Ping Liem and S. J. Webb, Supramolecular Chemistry of Membranes, in *Supramolecular Chemistry: From Molecules to Nanomaterials*, ed. P. Gale and J. Steed, Wiley-VCH Verlag GmbH & Co. KGaA, Weinheim, 2012.

9 (*a*) *Supramolecular Catalysis*, ed. P. W. N. M. van Leeuwen, Wiley-VCH Verlag GmbH & Co. KGaA, Weinheim, 2008; (*b*) *Molecular Encapsulation Organic Reactions in Constrained Systems*, ed. U. H. Brinker and J.-L. Mieusset, Wiley-VCH Verlag GmbH & Co. KGaA, Weinheim, 2010.

10 See for instance J.-M. Lehn, *Chem. Soc. Rev.*, 2007, **36**, 151–160.

11 B. C. Gibb, *Isr. J. Chem.*, 2011, **51**, 798–806.

12 (*a*) X. Zhang and C. Wang, *Chem. Soc. Rev.*, 2011, **40**, 94–101; (*b*) C. Wang, Z. Wang and X. Zhang, *Acc. Chem. Res.*, 2012, **45**, 608–618; (*c*) D. Myers, *Surfactant Science and Technology*, Wiley Interscience, New York, 3rd edn, 2005; (*d*) R. J. Farn, *Chemistry and Technology of Surfactants*, Blackwell Publishing, Oxford, 2006; (*e*) A. M. Carmona-Ribeiro, *Chem. Soc. Rev.*, 1992, **21**, 209–214.

13 (*a*) I. S. Shashikala and D. W. Bruce, *Dalton Trans.*, 2008, 1128–1131; (*b*) A. Santoro, A. M. Prokhorov, V. N. Kozhevnikov, A. C. Whitwood, B. Donnio, J. A. G. Williams and D. W. Bruce, *J. Am. Chem. Soc.*, 2011, **133**, 5248–5251; (*c*) F. Lesh, M. Allard, R. Shanmugam, L. Hryhorczuk, J. Endicott, H. B. Schlegel and C. N. Verani, *Inorg. Chem.*, 2011, **50**, 969–977; (*d*) H. Zheng and T. M. Swager, *J. Am. Chem. Soc.*, 1994, **116**, 761–762. For a recent review, see for instance: (*e*) C. A. Strassert, M. Mauro and L. De Cola, *Adv. Inorg. Chem.*, 2011, **63**, 47–103.

14 (*a*) See dedicated issue, ed. V. Balzani and S. Campagna, *Top. Curr. Chem.*, 2007, 280–281; (*b*) Y. Chi and P. T. Chou, *Chem. Soc. Rev.*, 2007, **36**, 1421–1431; (*c*) M. S. Lowry and S. Bernhard, *Chem. – Eur. J.*, 2006, **12**, 7970–7977.

15 (*a*) V. Fernández-Moreira, F. L. Thorp-Greenwood and M. P. Coogan, *Chem. Commun.*, 2010, **46**, 186–202; (*b*) M. Mauro, A. Aliprandi, D. Septiady, S. Kehr and L. De Cola,

Chem. Soc. Rev., 2014, **43**, 4144–4166; (*c*) U. Neugebauer, Y. Pellegrin, M. Devocelle, R. J. Forster, W. Signac, N. Moran and T. E. Keyes, *Chem. Commun.*, 2008, 5307–5309.

16 U. Hahn, H. Lülf, H. D. F. Winkler, C. A. Schalley, F. Vogtle and L. De Cola, *Chem. – Eur. J.*, 2012, **18**, 15424–15432.

17 S. Zanarini, E. Rampazzo, S. Bonacchi, R. Juris, M. Marcaccio, M. Montalti, F. Paolucci and L. Prodi, *J. Am. Chem. Soc.*, 2009, **131**, 14208–14209.

18 M. De Barros e Silva Botelho, J. M. Fernandez-Hernandez, T. Branquinho, H. Eckert, L. De Cola and A. S. Stucchi de Camargo, *J. Mater. Chem.*, 2011, **21**, 8829–8834.

19 (*a*) A. Guerrero-Martìnez, Y. Vida, D. Domìnguez-Gutiérrez, R. Q. Albuquerque and L. De Cola, *Inorg. Chem.*, 2008, **47**, 9131–9133; (*b*) D. Domìnguez-Gutiérrez, G. De Paoli, A. Guerrero-Martìnez, G. Ginocchietti, D. Ebeling, E. Eiser, L. De Cola and C. J. Elsevier, *J. Mater. Chem.*, 2008, **18**, 2762–2768.

20 (*a*) L. Zhao, K. M.-C. Wong, B. Li, W. Li, N. Zhu, L. Wu and V. W.-W. Yam, *Chem. – Eur. J.*, 2010, **16**, 6797–6809; (*b*) N. Liu, B. Wang, W. Liu and W. Bu, *J. Mater. Chem. C*, 2013, **1**, 1130–1136; (*c*) C. Po, A. Y.-Y. Tam, K. M.-C. Wong and V. W.-W. Yam, *J. Am. Chem. Soc.*, 2011, **133**, 12136–12143; (*d*) K. Wang, M. Haga, H. Monjushiro, M. Akiba and Y. Sasaki, *Inorg. Chem.*, 2000, **39**, 4022–4028.

21 (*a*) B. Kemper, Y. R. Hristova, S. Tacke, L. Stegemann, L. S. van Bezouwen, M. C. A. Stuart, J. Klingauf, C. A. Strassert and P. Besenius, *Chem. Commun.*, 2015, **51**, 5253–5256; (*b*) Y. R. Hristova, B. Kemper and P. Besenius, *Tetrahedron*, 2013, **69**, 10525–10533.

22 (*a*) M. P. Coogan, V. Fernández-Moreira, J. B. Hess, S. J. A. Pope and G. Williams, *New J. Chem.*, 2009, **33**, 1094–1099; (*b*) B. Manimaran, P. Thanasekaran, T. Rajendran, R.-J. Lin, I.-J. Chang, G. H. Lee, S.-M. Peng, S. Rajagopal and K.-L. Lu, *Inorg. Chem.*, 2002, **41**, 5323–5325.

23 (*a*) M. Mauro, G. De Paoli, M. Otter, D. Donghi, G. D'Alfonso and L. De Cola, *Dalton Trans.*, 2011, **40**, 12106–12106; (*b*) E. I. Szerb, A. M. Talarico, I. Aiello, A. Crispini, N. Godbert, D. Pucci, T. Pugliese and M. Ghedini, *Eur. J. Inorg. Chem.*, 2010, **21**, 3270–3277.

24 N. K. Allampally, C. A. Strassert and L. De Cola, *Dalton Trans.*, 2012, **41**, 13132–13137.

25 (*a*) W. Lu, S.-Y. Chui, K.-M. Ng and C.-M. Che, *Angew. Chem., Int. Ed.*, 2008, **47**, 4568–4572; (*b*) P. Besenius, G. Portale, P. H. H. Bomans, H. M. Janssen, A. R. A. Palmans and E. W. Meijer, *Proc. Natl. Acad. Sci. U. S. A.*, 2010, **107**, 17888–17893; (*c*) H. Dong, S. E. Paramonov, L. Aulisa, E. L. Bakota and J. D. Hartgerink, *J. Am. Chem. Soc.*, 2007, **129**, 12468–12472; (*d*) A. Ghosh, M. Haverick, K. Stump, X. Yang, M. F. Tweedle and J. E. Goldberger, *J. Am. Chem. Soc.*, 2013, **134**, 3647–3650; (*e*) C. Schaefer, I. K. Voets, A. R. A. Palmans, E. W. Meijer, P. van der Schoot and P. Besenius, *ACS Macro Lett.*, 2012, **1**, 830–833.

26 E. Ferri, D. Donghi, M. Panigati, G. Prencipe, L. D'Alfonso, I. Zanoni, C. Baldoli, S. Maiorana, G. D'Alfonso and E. Licandro, *Chem. Commun.*, 2010, **46**, 6255–6257.

27 (*a*) M. Panigati, M. Mauro, D. Donghi, P. Mercandelli, P. Mussini, L. De Cola and G. D'Alfonso, *Coord. Chem. Rev.*, 2012, **256**, 1621–1643; (*b*) M. Mauro, E. Quartapelle Procopio, Y. Sun, C. H. Chien, D. Donghi, M. Panigati, P. Mercandelli, P. Mussini, G. D'Alfonso and L. De Cola, *Adv. Funct. Mater.*, 2009, **19**, 2607–2614; (*c*) M. Mauro, C.-H. Yang, C.-Y. Shin, M. Panigati, C.-H. Chang, G. D'Alfonso and L. De Cola, *Adv. Mater.*, 2012, **24**, 2054–2058.

28 (*a*) E. Quartapelle Procopio, M. Mauro, M. Panigati, D. Donghi, P. Mercandelli, A. Sironi, G. D'Alfonso and L. De Cola, *J. Am. Chem. Soc.*, 2010, **132**, 14397–14399; (*b*) S. Tavazzi, L. Silvestri, P. Spearman, A. Borghesi, P. Mercandelli, M. Panigati, G. D'Alfonso, A. Sironi and L. De Cola, *Cryst. Growth Des.*, 2012, **12**, 742–749.

29 (*a*) M. R. Gill, J. Garcia-Lara, S. J. Foster, C. Smythe, G. Battaglia and J. A. Thomas, *Nat. Chem.*, 2009, **1**, 662–666; (*b*) E. Debroye and T. N. Parac-Vogt, *Chem. Soc. Rev.*, 2014, **43**, 8178–8192; (*c*) P. Besenius, J. L. M. Heynens, R. Straathof, M. M. L. Nieuwenhuizen, P. H. H. Bomans, E. Terreno, S. Aime, G. J. Strijkers, K. Nicolay and E. W. Meijer, *Contrast Media Mol. Imaging*, 2012, **7**, 356–361.

30 D. Donghi, G. D'Alfonso, M. Mauro, M. Panigati, P. Mercandelli, A. Sironi, P. Mussini and L. D'Alfonso, *Inorg. Chem.*, 2008, **28**, 4243–4255.

31 M. Rosso, A. T. Nguyen, E. de Jong, J. Baggerman, J. M. J. Paulusse, M. Giesbers, R. G. Fokkink, W. Norde, K. Schroën, C. J. M. van Rijn and H. Zuilhof, *ACS Appl. Mater. Interfaces*, 2011, **3**, 697–704.

32 J. Sauer, D. K. Heldmann, J. Hetzenegger, J. Krauthan, H. Sichert and J. Schuster, *Eur. J. Org. Chem.*, 1998, 2885–2896.

33 P. J. Giordano and M. S. Wrighton, *J. Am. Chem. Soc.*, 1979, **101**, 2888–2897.

34 L. A. Worl, R. Duesing, P. Cheng, L. Della Ciana and T. J. Meyer, *J. Chem. Soc., Dalton Trans.*, 1991, 849–858.

35 A. Cannizzo, A. M. Blanco-Rodriguez, A. El Nahhas, J. Sebera, S. Zalis, A. Vlcek and M. Chergui, *J. Am. Chem. Soc.*, 2008, **130**, 8967–8974.

36 (*a*) A. J. Lees, *Chem. Rev.*, 1987, **87**, 711–743; (*b*) P. Chen and T. J. Meyer, *Chem. Rev.*, 1998, **98**, 1439–1478; (*c*) R. A. Kirgan, B. P. Sullivan and D. P. Rillema, *Top. Curr. Chem.*, 2007, **281**, 45–100.

37 (*a*) M. Wrighton and D. L. Morse, *J. Am. Chem. Soc.*, 1974, **96**, 998–1003; (*b*) P. J. Giordano, S. M. Fredericks, M. S. Wrighton and D. L. Morse, *J. Am. Chem. Soc.*, 1978, **100**, 2257–2259; (*c*) A. Kumar, S.-S. Sun and A. J. Lees, *Top. Organomet. Chem.*, 2010, **29**, 1–35.

38 (*a*) G. Åkerlöf and O. A. Short, *J. Am. Chem. Soc.*, 1936, **58**, 1241–1243; (*b*) F. Hovorka, R. A. Schaefer and D. Dreisbach, *J. Am. Chem. Soc.*, 1936, **58**, 2264–2267; (*c*) L.-M. Omota, O. Iulian, O. Ciocirlan and I. Nita, *Rev. Roum. Chim.*, 2008, **53**, 977–988.

39 (*a*) J. N. Israelachvili, D. J. Mitchell and B. W. Ninham, *J. Chem. Soc., Faraday Trans. 2*, 1976, **72**, 1525–1568; (*b*) R. Nagarajan, *Langmuir*, 2002, **18**, 31–38.